

UCRL 8715

MASTER

UNIVERSITY OF
CALIFORNIA

Ernest O. Lawrence

*Radiation
Laboratory*

THE PRODUCTION OF NEUTRAL HYPERONS
BY 5-BEV π^- MESONS

BERKELEY, CALIFORNIA

DISCLAIMER

This report was prepared as an account of work sponsored by an agency of the United States Government. Neither the United States Government nor any agency Thereof, nor any of their employees, makes any warranty, express or implied, or assumes any legal liability or responsibility for the accuracy, completeness, or usefulness of any information, apparatus, product, or process disclosed, or represents that its use would not infringe privately owned rights. Reference herein to any specific commercial product, process, or service by trade name, trademark, manufacturer, or otherwise does not necessarily constitute or imply its endorsement, recommendation, or favoring by the United States Government or any agency thereof. The views and opinions of authors expressed herein do not necessarily state or reflect those of the United States Government or any agency thereof.

DISCLAIMER

Portions of this document may be illegible in electronic image products. Images are produced from the best available original document.

UCRL-8715
Physics and Mathematics

UNIVERSITY OF CALIFORNIA
Lawrence Radiation Laboratory
Berkeley, California

Contract No. W-7405-eng-48

THE PRODUCTION OF NEUTRAL HYPERONS
BY 5-BEV π^- MESONS

David Franklin Hotz
(Thesis)

April 13, 1959

Printed for the U. S. Atomic Energy Commission

THE PRODUCTION OF NEUTRAL HYPERONS
BY 5-BEV π^+ MESONS

CONTENTS

Abstract	3
I. Introduction	4
II. Experimental Method and Reduction of Observations	
Pion Beam and Apparatus	6
Film Scanning	12
Production-Plane Bias	14
Decay-Plane Bias	17
Detection Efficiency	20
Identification of Events	28
III. Results and Discussion	
Total Cross Section	29
The Λ Lifetime	33
Production Angular Distributions	36
The Center-of-Mass Distribution	36
The Laboratory Distribution	36
Decay Angular Distributions	38
The Up-Down Distribution	38
The Fore-Aft Distribution	40
The Λ Momentum Distribution	45
Production-Star Prong Distribution	45
Acknowledgments	48
Appendix	49
Bibliography	50

THE PRODUCTION OF NEUTRAL HYPERONS
BY 5-BEV π^- MESONS

David Franklin Hotz

Lawrence Radiation Laboratory
University of California
Berkeley, California

April 13, 1959

ABSTRACT

Neutral hyperons produced by 5-Bev π^- mesons incident on a large propane bubble chamber are analyzed in detail with respect to production cross sections and angular distributions of production and decay, and the Λ lifetime is measured. The cross section for neutral-hyperon (Y^0) production by the reaction $\pi^- p \rightarrow Y^0 K$ is 0.98 ± 0.16 mb. The cross section for carbon $\sigma(\pi^- C \rightarrow Y^0 K)$ is 6.05 ± 0.89 mb. The mean Λ decay time is $(3.12 \pm 0.34) \times 10^{-10}$ sec. The corrected lifetime is observed to be $(3.23 \pm 0.36) \times 10^{-10}$ sec. Although the up-down decay asymmetry for Λ hyperons is not significantly different from zero, the fore-aft decay angular distribution is asymmetric; a $\bar{P} = -0.31 \pm 0.12$ where the decay proton distribution along the Λ direction of motion has been examined. This is suggested as evidence for nonconservation of parity in the production interaction. The Λ -production angular distribution is peaked backward in the production center of mass. The Λ momentum spectrum and the distribution of Λ -production star prongs are presented. Sources of bias and their correction are discussed, and an estimate is made of the carbon contamination of the events that contribute to the hydrogen cross section for Y^0 production.

I. INTRODUCTION

The neutral V particles and their charged counterparts have been intensively studied ever since the original work of Rochester and Butler in 1947.¹ The early work was largely concerned with establishing the simple properties of these particles, such as Q values, lifetimes, and decay modes. Cosmic rays were the only source of these particles until accelerators were constructed that could accelerate protons to the energy range of 10^9 electron volts. It was soon found that the production of heavy unstable particles is "copious"² in $\pi^- p$ interactions, with a production cross section of one millibarn (mb) out of the total inelastic cross section of 25 mb at 1.4 Bev.³ The long lifetime of the particles in view of their copious production is understood by the hypothesis of associated production.⁴ The strange particles are produced in pairs via the strong interaction and decay independently via the weak interaction. This idea contains implicitly the notion that the production process is conserving some quantum number (strangeness quantum number) and leads to the introduction of the concept of strangeness.⁵

Recently developed experimental techniques such as the bubble chamber have aided the investigation of difficult and sophisticated problems in the study of strange particles. A survey of these experiments includes the production cross section near threshold⁶ and strong interactions with nucleons,⁷ the particle mixture concept⁸ and anomalous decays,⁹ the nonconservation of parity in the decay of strange particles,¹⁰ and determinations of intrinsic spin.¹¹ Interest in these particles stems from our relative ignorance of their properties and behavior under strong and weak interactions. It is interesting to remember that the π meson was discovered almost simultaneously with the V particles, yet present understanding of the strange particles is less developed than those corresponding levels of pion phenomena.

Much of the strange-particle production has been observed in bubble chambers of hydrogen or propane utilizing pion-proton interactions. The energies of the pion beams in these experiments were

all chosen in the vicinity of the strange-particle production thresholds ranging from a pion kinetic energy of 910 Mev to 1300 Mev. The analysis of experimental data and theoretical interpretation of the dynamics of production and decay are simplified considerably in dealing with final states of low relative energy. Because of low energy, the final state of two strange particles is well defined theoretically, and each identified V^0 possesses a unique momentum according to its angle of emission, because no other particles are produced. Thus in the production experiments in propane it is possible to make a reasonable separation between hydrogen events and carbon events and between the ΛK and $\Sigma^0 K$ final states. In this experiment an incident pion of 5 Bev releases a total energy of 3.2 Bev in the production center of momentum, and it is possible to produce a maximum of 12 pions in addition to a $K-Y$ pair. Here Y is the symbol for a hyperon. Obviously it is impossible to separate hydrogen events from carbon events by kinematic requirements, alone. Likewise it is not feasible to separate $\Sigma^0 K$ events from ΣK events. Therefore one finds the sum of cross sections $\pi^- p \rightarrow \Sigma^0 K$ and $\pi^- p \rightarrow \Lambda K$ and represents it as a single cross section $\pi^- p \rightarrow Y^0 K$. However, one is able to make a reasonable estimate of the carbon contamination as shown later.

The events described in this report were obtained by exposing a large propane (C_3H_8) chamber to a 5000-Mev π^- beam at the Berkeley Bevatron. A previous experiment utilizing a diffusion cloud chamber has been performed under similar conditions.¹² It also yielded data on V^0 angular distributions and a rough estimate of the Y^0 -production cross section at Bevatron energies.¹³ Three results are of particular interest here: (a) the production cross section of Y^0 's at high energies, (b) the appearance of an asymmetric fore-aft distribution in the decay of the Λ , and (c) a Λ lifetime in agreement with that observed in cosmic rays. The lifetime also agrees with that obtained in the Berkeley bubble chamber experiments.¹⁴

II. EXPERIMENTAL METHOD AND REDUCTION OF OBSERVATIONS

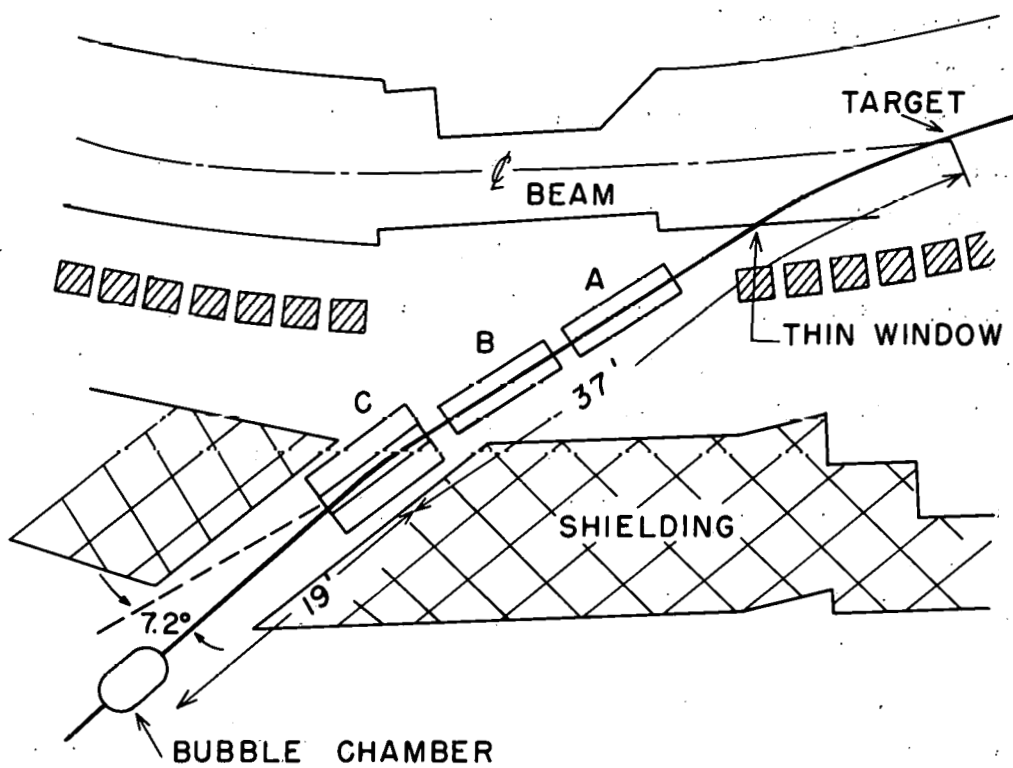
Pion Beam and Apparatus

The experimental arrangement is shown in Fig. 1. The circulating proton beam of 6.2-Bev kinetic energy struck a copper target at 14° preceding the west straight section. Particles leaving the target tangent to the proton beam were analyzed by the Bevatron field for a negative particle momentum of 5.5 Bev/c. Two successive quadrupole triplets (A and B) were used each as a single lens, and the beam was then deflected 7.2° by a 5-ft analyzing magnet (C). The center of the propane chamber was coincident with the target image, being located 56 ft from the target. The momentum of most pions fell between 5 and 5.5 Bev/c.

The beam was composed primarily of pions, with contaminations of μ^- mesons and electrons in decreasing order. Despite the distance of the chamber from the target, the high velocity of 5 Bev/c pions ($\beta\gamma \sim 36$) yields a calculated μ component of $(6 \pm 1)\%$.

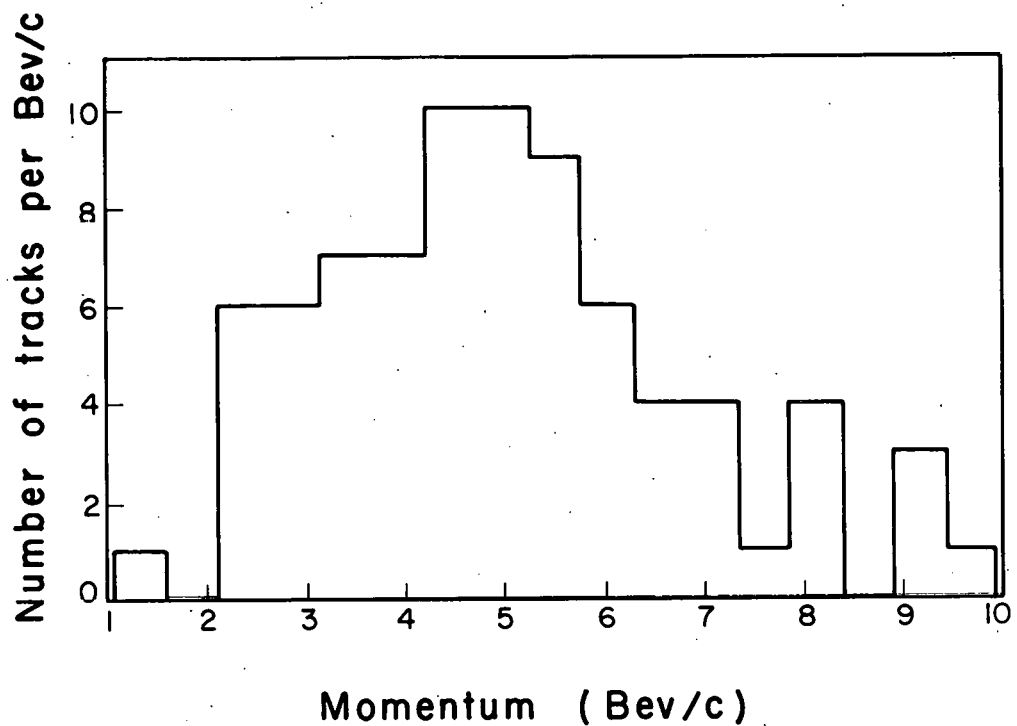
The electron component is negligible. The mean beam momentum incident on the chamber was determined by magnetic analysis and counter measurements to be 5.02 ± 0.25 Bev/c. Radius-of-curvature measurements on a selected sample of beam tracks (Fig. 2) yielded a mean momentum of 5.03 ± 0.21 Bev/c which is in good agreement with the independent determination by magnetic analysis. The value of the beam momentum is not critical in the analysis that follows. Consequently a value of 5.00 Bev/c was adopted in the subsequent calculations that require knowledge of this parameter.

The observations were made with a large bubble chamber of the propane type expanded ten times per minute in a constant magnetic field of 13,000 gauss (Figs. 3 and 4). The chamber and its associated equipment have been described previously.¹⁵ Photographs of the expanded chamber were obtained in stereo pairs by two cameras using Eastman Linagraph Panchromatic 70-mm film and equipped with matched wide-field Dagor lenses of 4-3/8-in. focal length. Fiducial marks consisted of a 5-cm grid on the top and bottom glasses of the chamber and auxiliary sets of crosses on both glasses. Picture number, perinent run data, and magnet current indicated on an ammeter were recorded on each photograph.



MU-16376

Fig. 1. The beam setup showing location of magnets and chamber.



MU-17127

Fig. 2. Distribution of measured momenta of pion beam tracks.

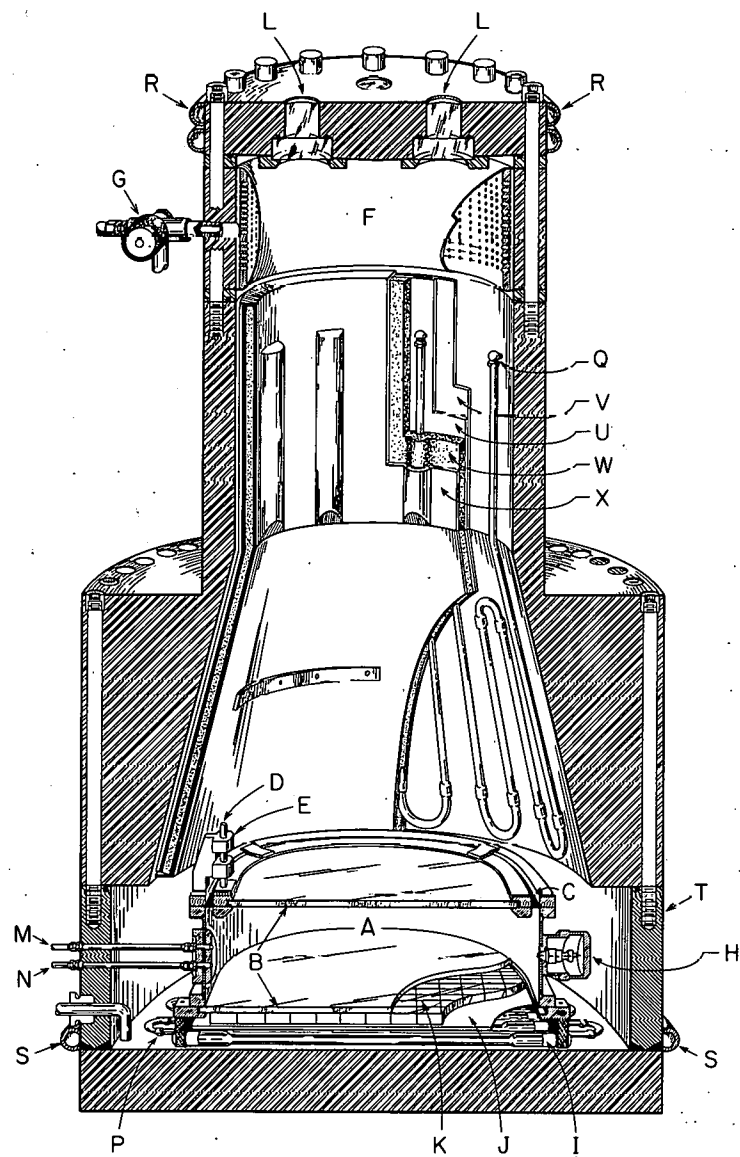
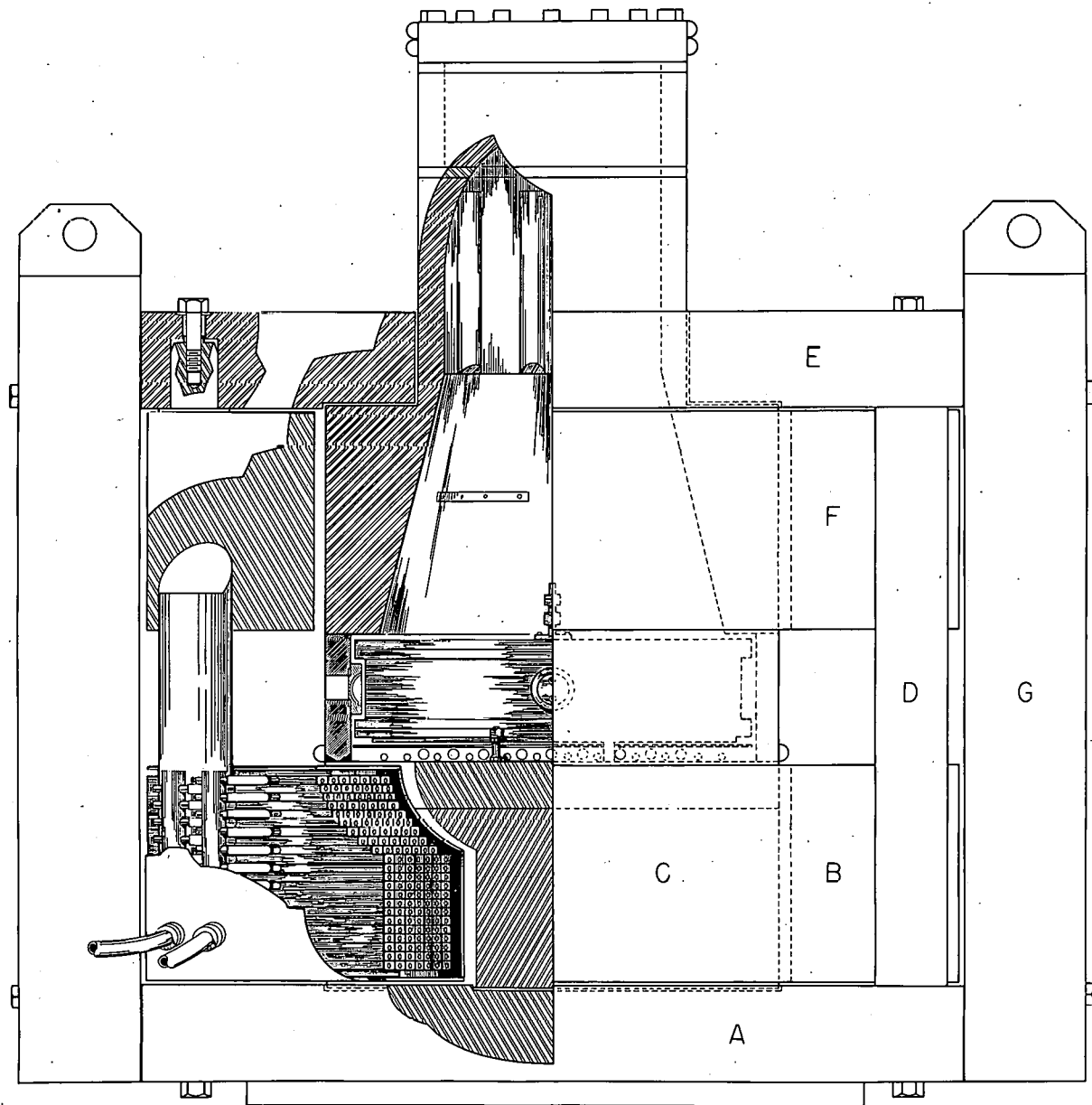


Fig. 3. The 30-inch propane bubble chamber, showing
(a) the propane container, (b) the glass windows,
(c) flexible rubber diaphragm between side wall
and top-glass clamping ring, (d) stainless steel
guiding rod, (e) cylindrical ball bearings controlling
the guiding rod, (f) cylindrical Hycar rubber
diaphragm, (g) 3/4-in. Barksdale valve,
(h) transducer for measuring the propane
pressure, (i) one of the 13 flash tubes, (j) opal-
glass diffuser, (k) venetian-blind light collimator,
(l) two of the four viewing ports in the top of the
chamber, (m) thermocouple for measuring the
propane temperature, (n) propane fill tube,
(p) water tubes under the chamber, (q) water
tubes in the upper part of the oil container,
(r) water tube around the top cover plate,
(s) water tube around the bottom of the oil container,
(t) nonmagnetic steel region, (u) copper sheet,
(v) Mylar sheet, (w) polyurethane sponge, and
(x) copper sheet.



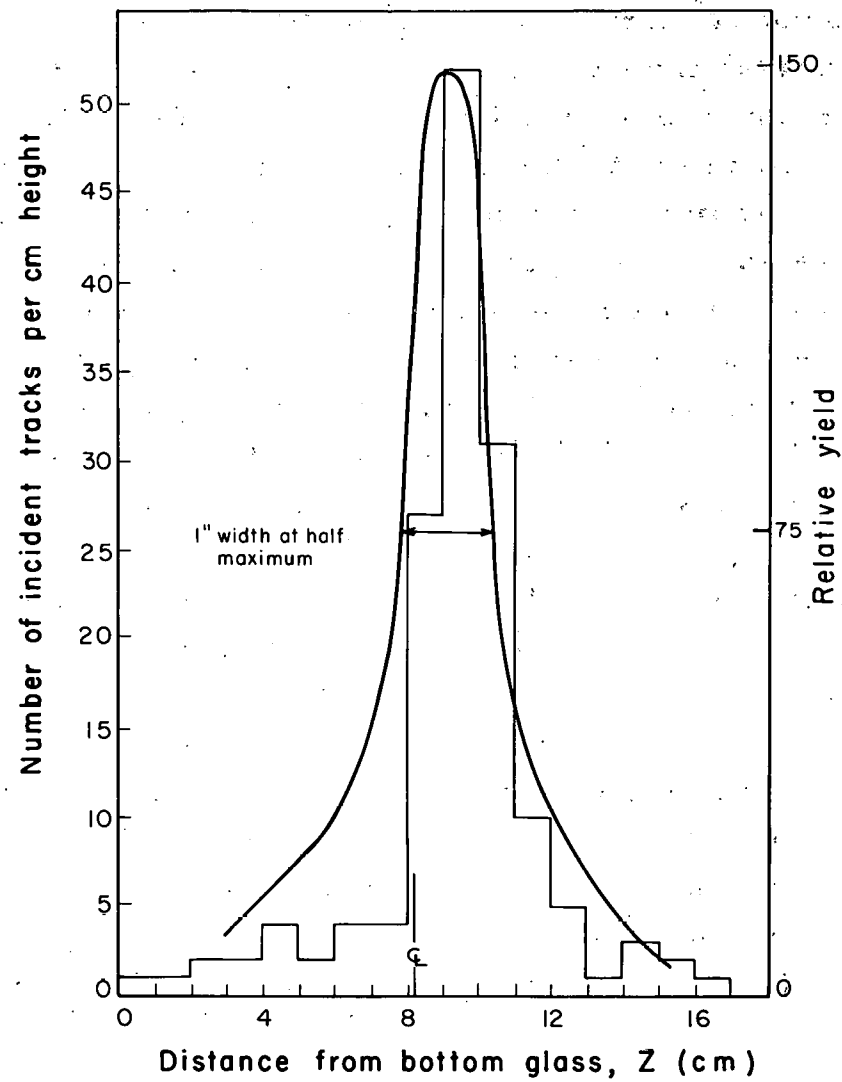
MUB-198

Fig. 4. The 30-inch propane bubble chamber in its magnet, showing (a) iron slab forming the bottom of the magnet, (b) bottom copper coil, (c) iron cylinder, (d) four iron posts supporting top slab E, (e) upper iron slab, (f) upper coil of the magnet, and (g) return paths.

Film Scanning

About 30,000 pictures were obtained and scanned once in a group effort to find V^0 particles, Ξ particles, and antihyperons. Ten thousand of the highest quality pictures were selected for a second scan. The second scan was principally devoted to searching for V^0 production by beam pion interactions in the visible propane volume. We may estimate the scanning efficiencies by comparing the results of the two separate scans. If N is the number of recognizable events, then n_1 events are found in the second scan with efficiency $e_1 = n_1/N$ and n_2 events are found in the second scan with efficiency $e_2 = n_2/N$. The number of recognizable events found in a double scan is $n = n_1 + n_2 - n_{12}$, where n_{12} is the number of events found in common to both scans. The joint efficiency of a double scan is given by $e_{12} = 1 - (1 - e_1)(1 - e_2)$. The second scan of 10,000 selected pictures gave $e_1 = e_2 = 74\%$ and a joint efficiency of 93% in finding a recognizable V^0 decay with a possible related production origin nearby.

The depth dependence of scanning efficiency can be important if the vertical dimension of the beam is comparable to chamber depth or the beam is off center. Figure 5 shows the depth distribution of production origins, which is in excellent agreement with the beam profile determined by counter measurements. A depth correction to scanning efficiency for finding the origins is therefore negligible.

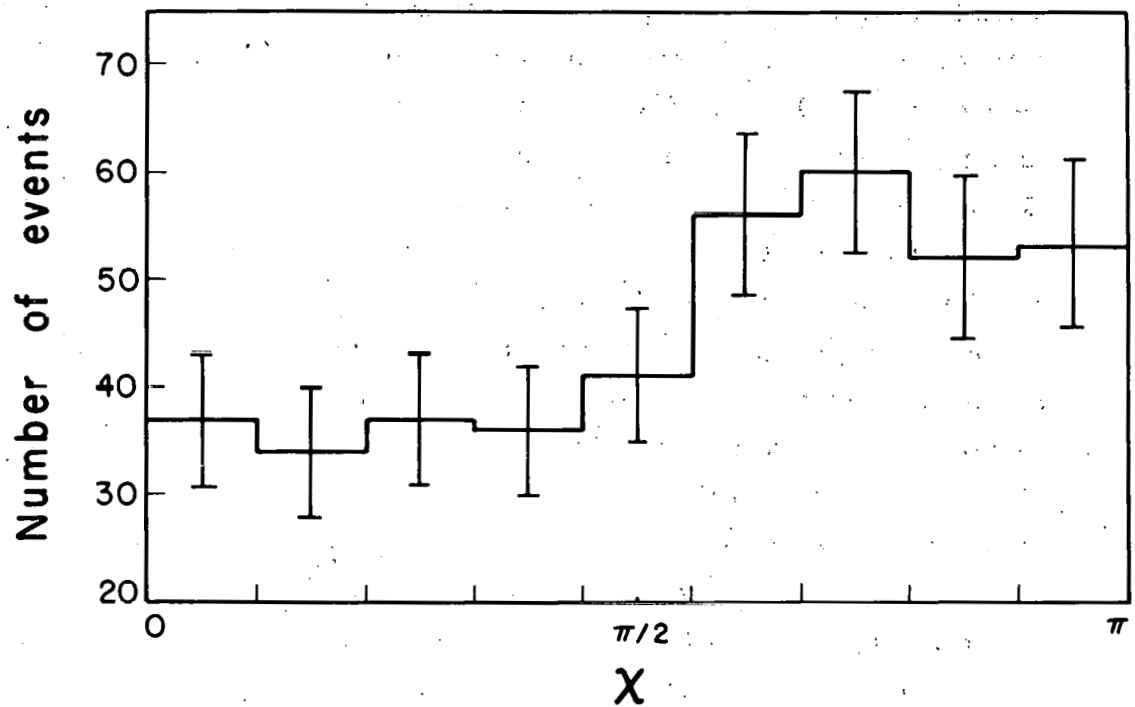


MU-17133

Fig. 5. Height distribution of V^0 production origins.
Smooth curve is flux in 1-in. by 1-in. counters.
The histogram is derived from measured
origins.

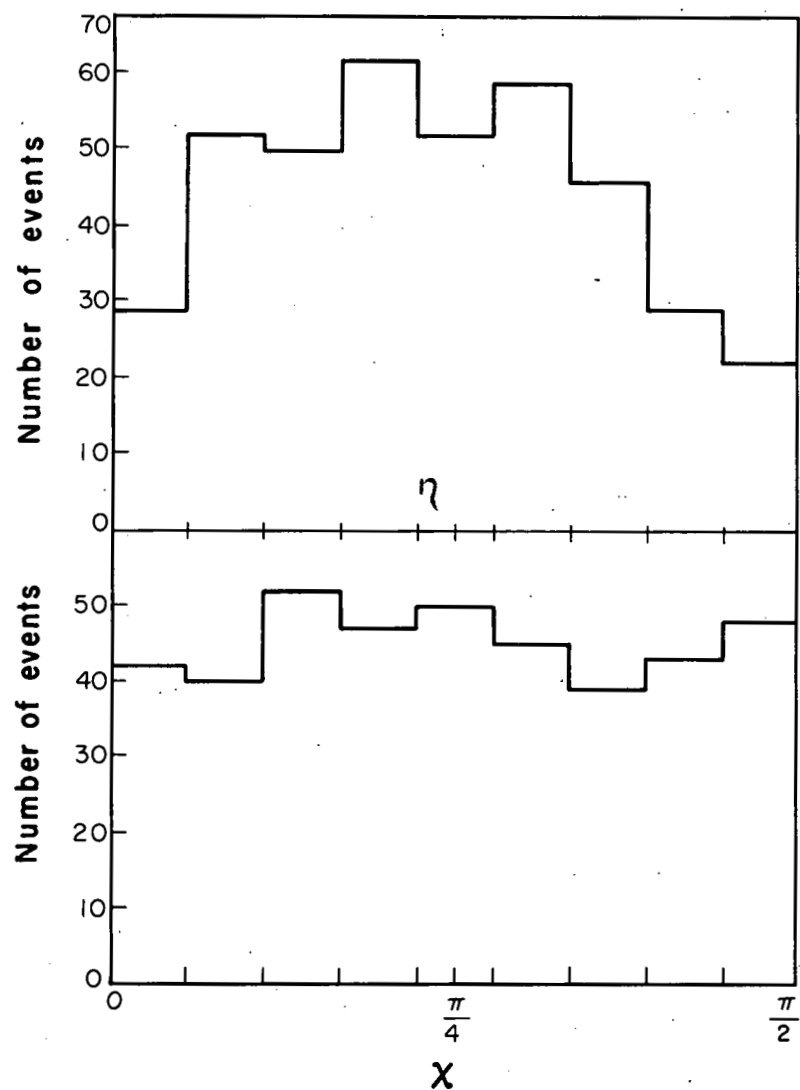
Production Plane Bias

A chamber with a sensitive depth that is shallow compared to its width and length can effectively create a bias against observing events with vertical production planes. This bias against observing a particular production-plane orientation is enhanced by an asymmetric lateral distribution of the pion beam. Although the beam is well focused vertically, its lateral distribution across the chamber rises from zero along the left wall to a maximum flux along the right wall of the chamber. Consequently V^0 particles are missed when they are produced near the right side and subsequently come off to the right. Figure 6 shows the distribution for all V^0 particles observed, where χ is the angle between the production plane normal and the vertical normal parallel to the magnetic field. The χ distribution should be isotropic. The asymmetric beam distribution causes some V^0 particles with production planes near zero to be missed. The diminution of V^0 observed with production planes near 90° is because the chamber has more area than depth. Thus from the folded χ distribution of Fig. 7a one may estimate that 84% of the V^0 particles were observed, and therefore 16% of the Λ^0 sample was missed because of production-plane bias.



MU-17135

Fig. 6 Distribution in production-plane orientation χ for all observed V^0 .



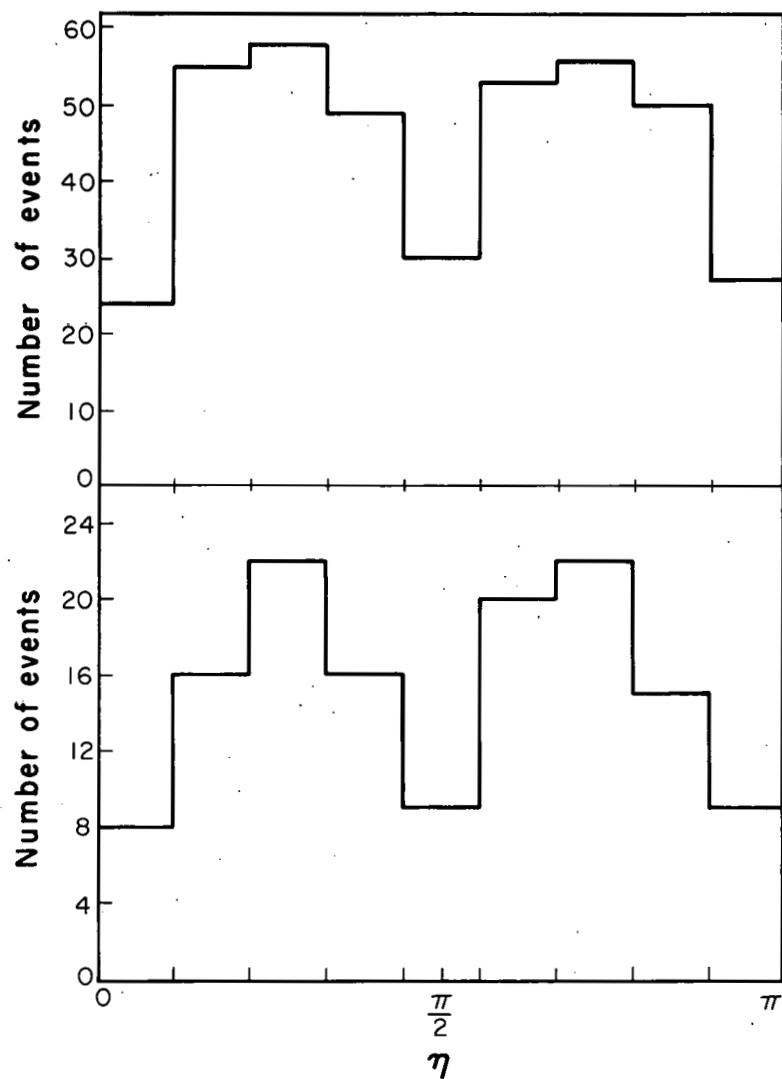
MU-17128

Fig. 7 (a) Folded distribution in production-plane orientation χ for all V^0 . (b) Folder distribution in decay-plane orientation η for all V^0 .

Decay-Plane Bias

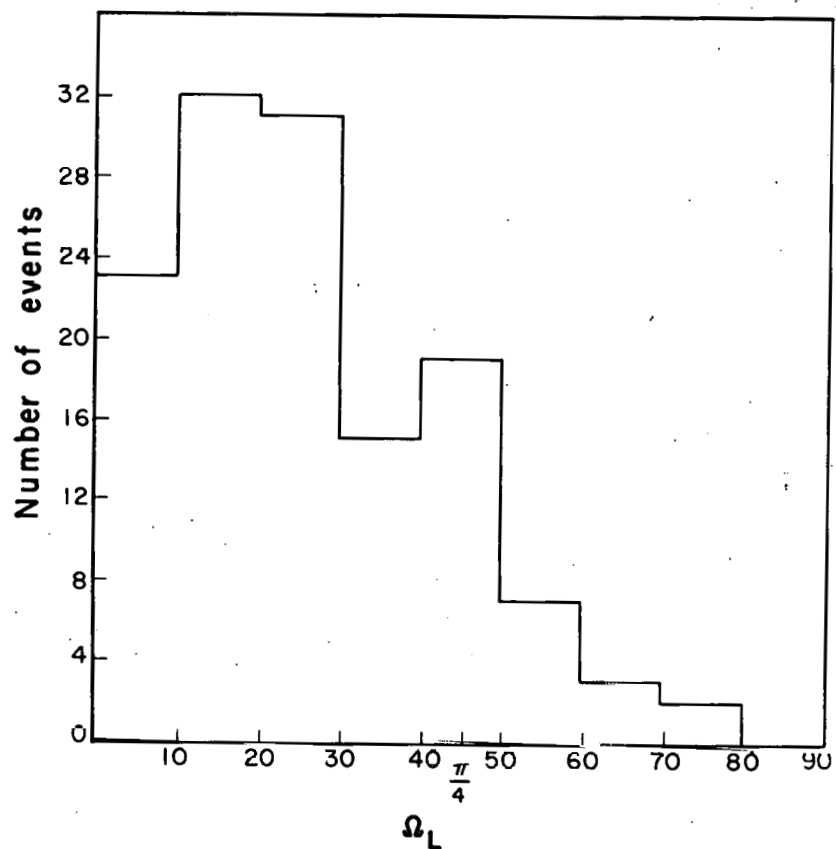
The angular distribution of V^0 decay planes with respect to the plane of the chamber is shown in Fig. 8a. The corresponding distribution for all observed Λ hyperons is shown in Fig. 8b. The independent variable η represents the angle between the decay plane normal and the vertical direction to the chamber plane. Both distributions are of the same form which is approximately $1 + \sin 2\eta$. The following discussion explains why this is the distribution expected.

The suppression of observed decay planes near zero is dependent on the production angular distribution in the laboratory system. The minimum angle η' that a decay plane can make with the plane of the chamber is the angle that the V^0 line of flight forms with a horizontal plane. Consider the folded η distribution of Fig. 7a for all V^0 's. Those V^0 's forming an angle η' with the chamber plane can decay with η values from η' to $\pi/2$. The range $0 \leq \eta \leq \eta'$ is physically impossible, since the decay plane must contain the direction of the V^0 . This does not imply that the suppression of decays with η values near zero represents missed decays. The number of decays with η near $\pi/2$ should be roughly equivalent to those with η near zero. One can see this by examining those V^0 's that come off in the plane of the chamber and hence are free to decay with η values from 0 to $\pi/2$. The Λ laboratory production angular distribution is shown in Fig. 9. It is approximately a $\cos^2 \Omega_L$ distribution where Ω_L is the laboratory production angle. This is a factor in suppressing the η distribution near $\pi/2$. The fact that the distribution obtained is that expected indicates that the decay-plane distribution is free from bias.



MU-17124

Fig. 8. (a) Distribution in decay-plane orientation η for all observed V hyperons. (b) Distribution in decay-plane orientation η for all observed Λ hyperons.



MU-17126

Fig. 9. Distribution of laboratory production angles for observed Λ hyperons.

Detection Efficiency

Production events of V^0 are found by scanning first for the characteristic decay and then attempting to find a production origin in the chamber volume of propane. In the course of identification of these V events as legitimate, they are subjected to the constraint that their transverse momentum must balance about the assumed line of flight defined by the production and decay points. This procedure eliminates practically all the anomalous decays. The leptonic decays have been shown to be less than 2% and consequently are neglected.¹⁷ This procedure of finding a decay and its production origin selects a sample of V particles from a background of similar particles produced in the steel chamber walls and accidental neutron stars.

One can lose real events in the following ways:

- (a) the decay is visible as a recognizable V but is overlooked,
- (b) either the decay or its related production origin is obscured because of an excess of tracks in the chamber,
- (c) the decay event is invisible because of decay via a neutral or long-lived mode,
- (d) the V decays outside the visible region of the chamber, and
- (e) the V decays via the charged mode in the visible region, but is not recognized as a legitimate decay.

Such losses of events were compensated for in the following ways. (a) The recognizable events lost by inefficient scanning and the resultant correction have been discussed under Film Scanning. (b) Pictures with too many tracks were eliminated in a systematic way by counting beam plus background tracks crossing any 25-cm length perpendicular to the beam axis. When this count was \geq 45, the picture was rejected. This eliminated those decays in which the production origin was obscured because of an excessive number of tracks in the upstream region. (c) The branching ratio for charged decay of Δ particles was taken to be 63%.¹⁸ (d) The probability of observing a V^0 decay via its charged mode depends on the particle's lifetime, momentum, and geometrical factors. Gayther and Butler¹⁹ give a simple expression that allows a correction to be made for those that decay via the charged mode outside the observable region. The

probability of decay in the visible region is $P(t_0, T) = e^{-t_0/\tau} e^{-T/\tau}$ where the time ratios refer to the same frame of reference, t_0 is the time of flight from the production point to the point where the decay can first be observed, and T is the maximum time of flight from the production point to the exit point from the fiducial volume. The exponents are of the form

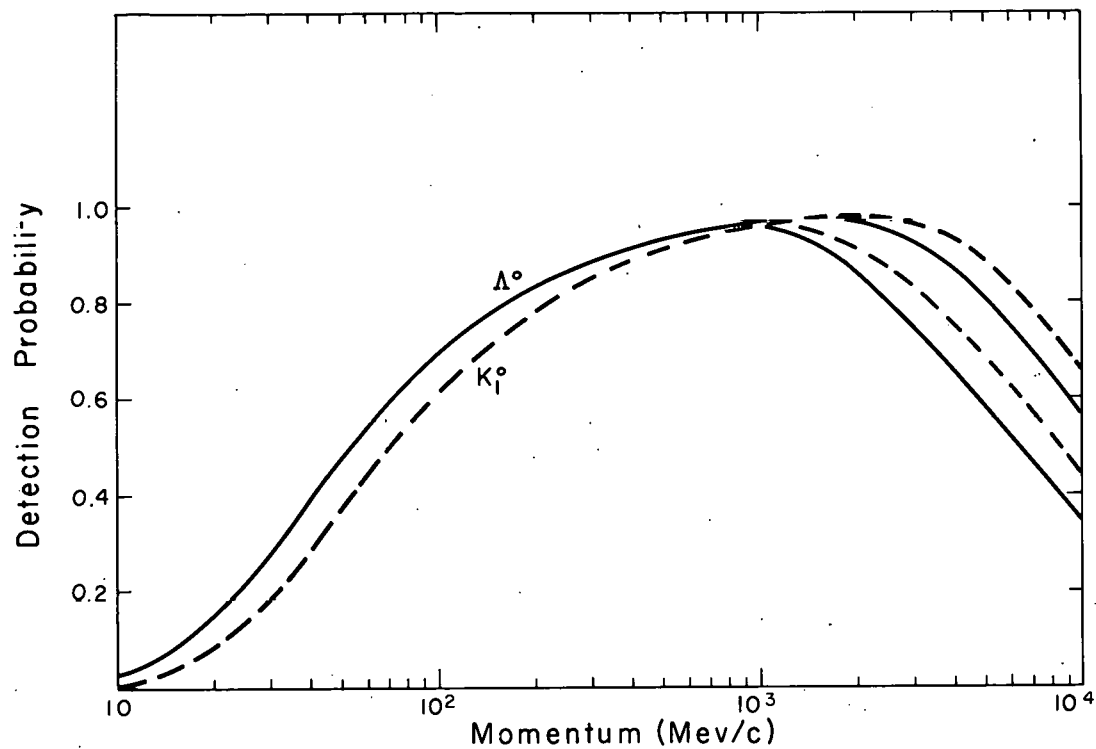
$$t_0/\tau = \frac{m}{c\tau} \frac{a}{p}, \quad T/\tau = \frac{m}{c\tau} \frac{L}{p},$$

where a is a fixed distance necessary in order that a V particle get sufficiently far from a production origin to be distinguishable from two prongs of the production star. It is taken to be 3 mm, which is about the range of a μ^+ in propane from π^+ decay. Here $L+a$ is the distance along the flight line from production origin to the intersection with a surface of the fiducial volume, the V^0 momentum is p , and τ_Λ was taken to be 3×10^{-10} sec and τ_θ as 1×10^{-10} sec in calculating $P(t_0, T)$.

As an example, the detection probability $P(t_0, T)$ is shown as a function of momentum in Fig. 10 for both V^0 types. The value of $P(p)$ was calculated for $L = 35$ cm, an average potential path, and for $L = 66$ cm, a maximum potential path. The graph shows that $P(p)$ is insensitive to L changes up to about $p = 1$ Bev/c. Beyond that, greater L values increase the detection probability.

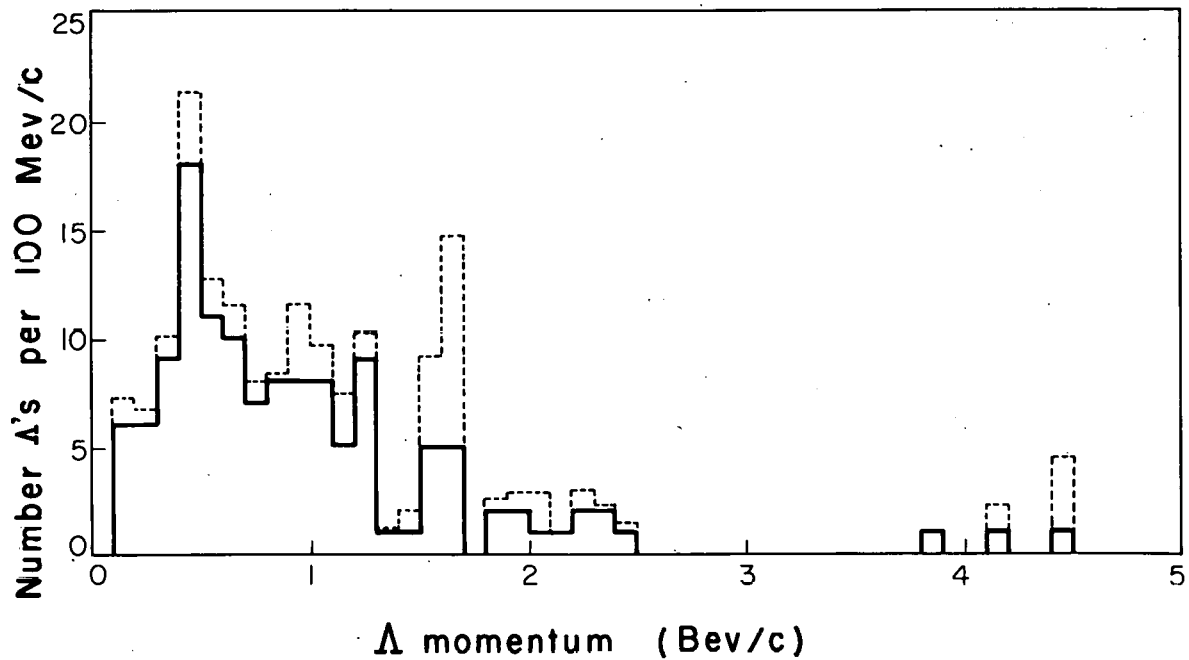
This technique is used in correcting the Λ^0 momentum spectrum (Fig. 11). By the method of Gayther and Butler, each observed event is given a weight of $W \equiv (1/P)$. This corrects for those events decaying outside the fiducial region.

There is another method one can use to correct for decays out of the visible region when a well-defined beam and visible production origins are available in a large chamber. The V^0 decays are lost because of edge effects and production-plane bias. The correction for production-plane bias has already been discussed. The correction for depth dependence of scanning has been discussed and found to be negligible. The correction for edge effects along the side walls of the



MU-17187

Fig. 10. Detection efficiency of the 30-in. bubble chamber.



MU-17125

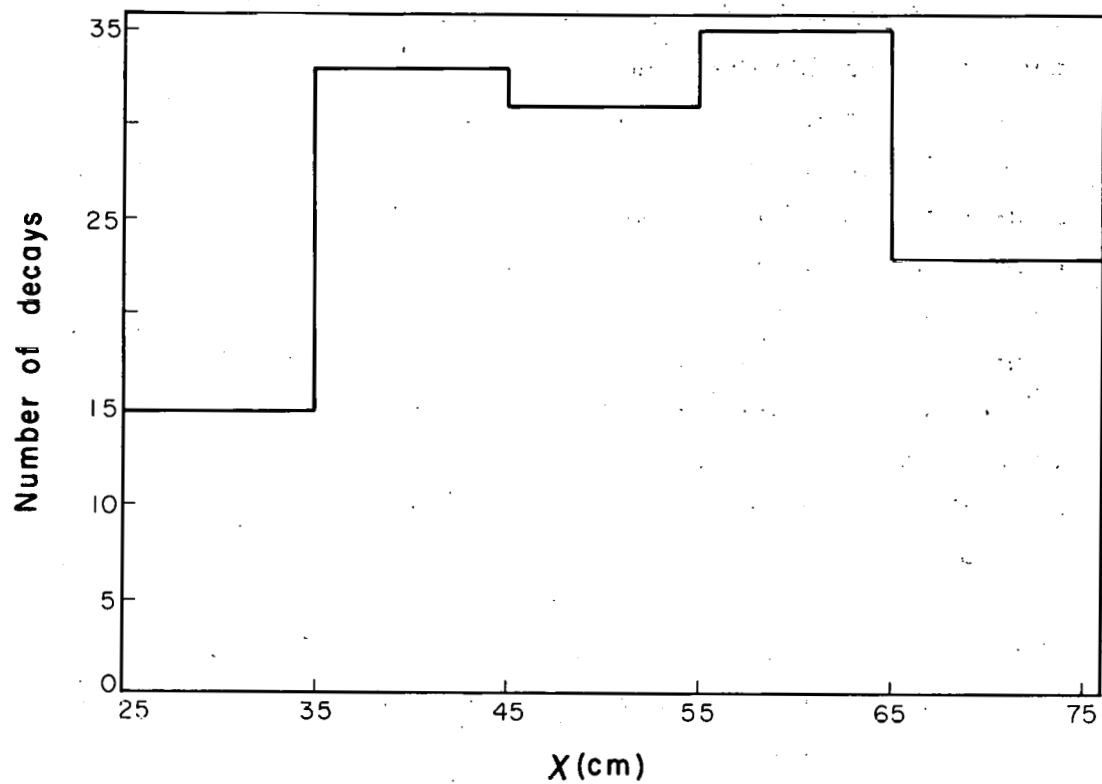
Fig. 11. The Λ momentum distribution. The solid line is the observed number, the dotted line is the weighted number.

chamber are included in the correction due to production-plane bias. The loss due to the ends of the chamber is the only correction that remains. The number of observed Λ decay origins as a function of x (the beam distribution) is plotted in Fig. 12. Λ decays are missed near the front wall of the fiducial region ($x = 25$ cm) because the production is outside the fiducial region. The Λ decays are missed near the end wall ($x = 75$ cm) because the decay is outside the fiducial volume for production just inside the end wall. However those decays missed near the front wall are not to be considered as a correction, because their production was outside the fiducial region. Those decays missed near the end wall are considered as a correction to the number of observed Λ 's for cross section purposes. The cross section for Y^0 production is derived from those production events in the fiducial volume. If the distribution of decays is assumed constant along the beam direction, then the observed sample of Λ decays in Fig. 11 represents 93% of the Y^0 hyperons produced in the fiducial region.

One can check the correction for the end-wall effect and the production-plane bias by comparison with the weighting factor of Gayther and Butler. The production-plane and end-wall bias combined indicate that $(79 \pm 7)\%$ of the Λ decays are observed. The weighting factor applied to the observed decays shows that $(75 \pm 9)\%$ of the Λ decays are observed. The agreement between the two methods of correction is well within experimental error.

(e) There are two factors contributing to this bias. As is well known, V^0 particles with decay planes nearly parallel to the lens axis through which they are being observed are more difficult to detect in scanning than those with decay planes perpendicular to this axis. The strong magnetic field and the long track lengths effectively remove this bias, as was shown in the discussion of decay-plane bias.

The second factor contributing to the bias of type (e) arises when a decaying Λ hyperon emits a low-energy negative pion in the laboratory. One requirement in scanning was that the V^0 decay exhibit a definite negative prong. A range of 1 cm in propane was taken as a lower limit on the negative prong. If the negative pion formed a



MU-17121

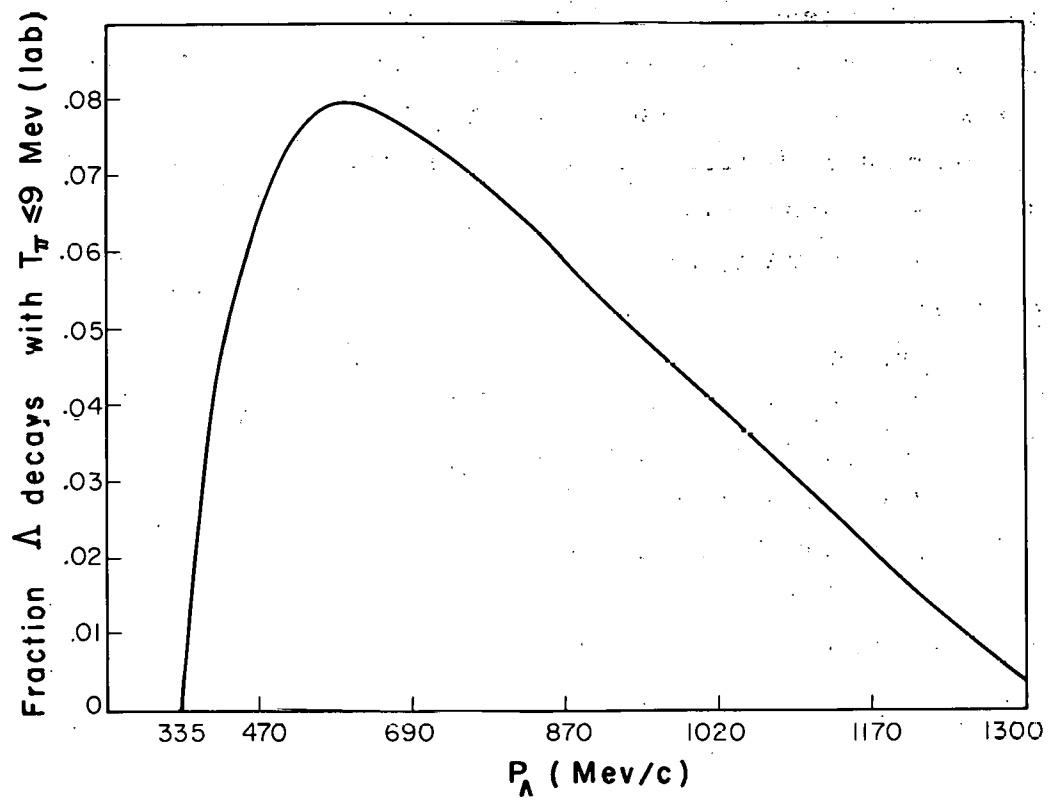
Fig. 12. Distribution of the Λ decays along the beam.

prong of 1-cm length or less the event was discarded. This effect is enhanced in propane, since a pion with an energy of 9 Mev will travel only 1 cm or less, and the observed positive track is easily confused with the effects of the neutron background. If one assumes isotropic decay in the center of mass, the fraction of Λ 's of a given momentum which has π^- mesons with ranges less than 1 cm in the laboratory system is given by the curve of Fig. 13. By folding this curve into the momentum distribution of the Λ 's, the percentage of Λ hyperons discarded is found to be 7%.

In summary, these corrections to the Y^0 cross section are as follows:

(a) joint-scanning efficiency (e_{12})	93 ± 7 %
(c) fraction of charged decay	63 %
(d) production-plane bias	85 ± 5 %
(e) low-energy π^- bias	93 %.

The combined product of these correction factors gives an observational efficiency of 43.0%, which is used to correct the Y^0 cross section.



MU-17132

Fig. 13. Fraction of Λ decays with $T_\pi \leq 9$ Mev lab as a function of Λ momentum.

Identification of Events

An event was called a V^0 if it consisted of two prongs, one of which was negative. A V^0 was measured if a pion interaction could be associated with it as a production origin. Such an event was subsequently measured in both views by the use of a digitized microscope that yielded coordinates along a track in punched-card form. This data was processed on an IBM-650 computer to yield track momentum and direction (dip and azimuth angles) with their associated errors. The coordinates of the production and decay points were given. The range of tracks stopping in the liquid and the length used in determining angles and momenta were indicated for all tracks. The computed momentum errors allowed an additional 10% for multiple scattering in propane.

Some V^0 were identified in scanning, either by ionization estimates or by the fact that the positive track of the V^0 stopped in the chamber or interacted in the propane. For those V^0 particles that could not be identified by inspection, a Q value was calculated by first assuming a Λ decay and then a K^0 decay. If the calculated quantity $Q(\pi, p) \pm \delta Q$ included 38 Mev and $Q(\pi, \pi) \pm \delta Q$ did not include 214 Mev, the event was classed as a Λ , and vice versa for the K^0 decays. If the calculated Q values and their respective error intervals included 38 Mev and 214 Mev, the event was classed as an indistinguishable Λ - θ event. A few events which satisfied none of these conditions were apportioned in the same way by relaxing the Q limits to $Q \pm 2\delta Q$. This class of events was almost always composed of poorly measurable decays; both legs were short in the visible region and gave poorly determined momenta from curvature measurements, or small-angle scatters occurred which distorted the curvature and resulted in very inaccurate momentum values.

For practical purposes, it was always obvious in scanning which pion interaction was associated with an observed V^0 decay. However, a check on this question utilized a constraints calculation that balanced components of the resultant V^0 momentum about the line of flight by adjusting the measured momentum and direction of the V^0 legs. A maximum momentum unbalance of 10 Mev/c was permitted for each component. All origins assigned to V^0 particles in scanning were consistent with these constraints.

III. RESULTS AND DISCUSSION

Total Cross Section

A fiducial volume was selected in the chamber for total-cross-section and mean-life determinations. The volume measured 14 cm high, 40 cm wide, and 50 cm in length along the beam. Only those events that included the production origin and its decay Λ^0 within this volume were considered for analysis. To find a Λ^0 cross section, one needs to know the actual path traversed in the target by beam pions and the number of Λ produced. It can be shown that the average beam pion entering the chamber traversed an effective length $\lambda_T (1 - e^{-a/\lambda_T})$ before interacting, where a is the maximum length it could traverse and still produce a visible interaction, and λ_T is the mean free path for 5-Bev pion interactions of all kinds in propane.²⁰ The beam was sampled by counting in every twenty-fifth acceptable picture the number of beam tracks that entered the fiducial volume within $\pm 5^\circ$ of the mean beam direction. Tracks that suffered sudden changes in curvature were classed as electrons and were not counted. The average number of entering tracks times the number of acceptable pictures gives the number of entering pions. This product multiplied by $\lambda_T (1 - e^{-a/\lambda_T})$ gives the total path traversed by the beam, which amounts to 1.094×10^6 gm/cm² if the propane density is assumed to be 0.415 gm/cm³. The various factors that correct the observed number of Λ particles have been discussed under Experimental Method.

The high incident-pion energy and the resultant multiplicity of final states available make it impossible to separate carbon events from free-proton events by a kinematical analysis. Likewise Σ^0 production cannot be distinguished from direct Λ production because the momentum is not unique for a given production angle. Thus the cross section found here will represent that for both Λ and Σ^0 hyperons together. The method used to distinguish hydrogen events from carbon events is outlined below.

Production stars for Λ 's were divided into three classes. Production stars with slow prongs were not used in this estimate. The number of those with an even number of fast prongs was $N(\text{even})$ and those with an odd number of fast prongs, $N(\text{odd})$. A previous experiment with 5-Bev pions on hydrogen has shown that hydrogen events consist entirely of stars with an even number of fast prongs.¹² Therefore, all the hydrogen events are contained in $N(\text{even})$. There are also events produced in carbon, and the number of those carbon events with even numbers of fast prongs is indicated by $N(C)$. If $N(C)$ were known, then the number of hydrogen events $N(H)$ would be equal to $N(\text{even}) - N(C)$.

In order to estimate $N(H)$ the assumption is made that $N(C) = N(\text{odd})$. On the basis of this assumption, it is found that the carbon contamination is $(26 \pm 11)\%$.

The justification for this assumption lies in the fact that 5-Bev pions on hydrogen produce only even numbers of fast prongs, that the π^- -p and π^- -n total cross sections at 4.5 Bev are approximately equal,²¹ and that a π^- -n event would produce an odd number of fast prongs only. Thus with these assumptions, the collision of pions with quasi-free nucleons near the surface of the carbon nucleus should give even numbers of fast prongs for a proton and odd numbers of fast prongs for a neutron. For collisions with nucleons deeper in the nucleus or secondary reactions of mesons in the nucleus; boil-off protons would be expected to appear as slow prongs, and these events are excluded by the requirement of fast prongs only. Assuming that the corresponding set of Λ - θ indistinguishables divide in the same ratio as the distinguishables implies that 43% of the Λ - θ events are to be classed as Λ 's. Thus one finds:

joint scanning efficiency (e_{12})	$(93 \pm 7)\%$
fraction of charge decay	63%
low-energy π^- bias	93%
end-wall effect	$(93 \pm 5)\%$
production-plane bias	$(85 \pm 5)\%$
observed	$68 \pm 12\%$
carbon	$(26 \pm 11)\%$
beam-path length	$1.094 \times 10^6 \text{ gm/cm}^2 \pm 6\%$

$$\sigma = \frac{74(68)}{8(\frac{6.02}{44})(1.094)(0.43)} \times 10^{-29} \text{ cm}^2$$

$$= 97.5 \times 10^{-29} \text{ cm}^2$$

$$\sigma(\pi^- p \rightarrow K\Lambda^0) = 0.98 \pm 0.16 \text{ mb}$$

The sum of the cross section $K\Lambda$ and $K\Sigma^0$ at the highest energy measured thus far (1300 Mev) is 0.56 ± 0.18 mb.²² This high cross section at 5 Bev may be an indication that other channels contributing to the observed Λ may have opened because of the high energy available in the center of mass. Since only two Ξ^- hyperons were observed in this film,¹⁶ and because there is no obvious reason why Ξ^0 production should be much stronger than that for Ξ^- , it is impossible that Ξ^0 decay could produce a significant contribution to the Σ^0 cross section. It has been suggested that the exchange reaction $\Sigma^- p \rightarrow \Lambda n$ could contribute,²³ but this requires production in complex nuclei, and it is believed that the selection of events has eliminated this possibility. The increase of the cross section over that at 1300 Mev could be considered as evidence for an incorrect estimate for the carbon contamination, were it not for the fact that it is in rough agreement with that determined by Eisler et al. at 1300 Mev.⁶

An additional check on the determination of carbon contamination is provided if we assume an $(A)^{2/3}$ law for production and find the per nucleon cross section of propane for Σ^0 production by 5 Bev pions. Thus we have

$$\sigma(Y^0)/\text{nucleon} = \frac{167}{(1.094)(0.43)(\frac{6.02}{44})(23.75)} \times 10^{-29} \text{cm}^2$$

$$=(1.09 \pm 0.14) \text{mb/nucleon}.$$

The fact that this value is slightly larger than the cross section for free protons is in agreement with the greater transparency of the carbon nucleus at higher energies. It is also in agreement with the fact that inelastic pions are produced with energies above the associated production threshold. These additional pions can interact, producing strange particles before escaping the carbon nucleus and thus enhancing the production of neutral hyperons on carbon.

If we assume the validity of the contamination estimate, the carbon cross section for Y^0 production by 5-Bev pions is

$$\sigma(\pi^- C \rightarrow Y^0 K) = \frac{117}{(0.43)(1.094)(\frac{6.02}{44})(3)} \times 10^{-29} \text{cm}^2$$

$$=(6.05 \pm 0.89) \text{mb}.$$

For convenience, a list of events used to determine these quantities is listed below:

Number of Λ events from even fast-prong stars	58
Number of indistinguishable events from even fast-prong stars	24
Number of Λ events from all types of production stars	138
Number of indistinguishable events from all types of production stars	67
Number of θ_{-1}^0 events from all types of production stars	183

The Λ Lifetime

The Λ lifetime is of some interest because of the difference between values obtained mainly from Λ decays observed in cosmic rays and some values obtained in threshold experiments using accelerators. The accelerator results for the mean life are generally smaller than the cosmic ray values. (See Appendix 14). The experimental conditions of these conflicting measurements are usually quite different. The cosmic ray experiments presumably utilize high-energy pions incident on complex nuclei to produce neutral hyperons. The production is usually not observed directly. The accelerator experiments use well defined π beams of energy just above the associated production threshold. The strange particles are largely produced in simple pion-nucleon interactions, and the production origin is observed directly.

The accuracy of this lifetime measurement is insufficient to distinguish between the different values found. However, this measurement is of some value in that it simulates a well-controlled cosmic ray experiment, since the incident-pion energy is high, and most of the production occurs on complex nuclei (carbon). An additional improvement is that the production origin is always observed directly.

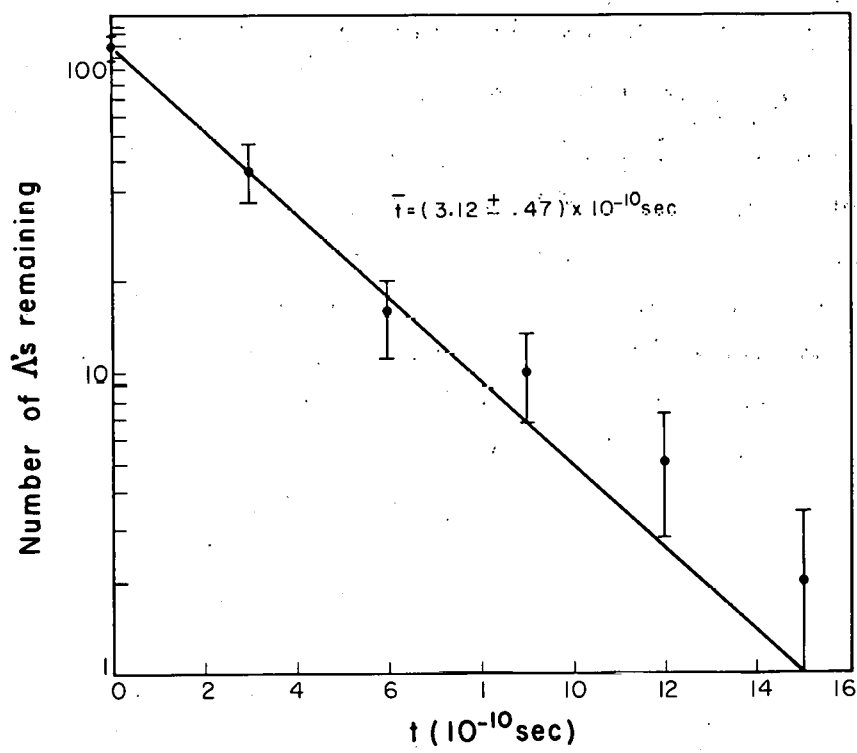
The technique used here is standard. ²⁴ If the Λ is produced at the point P and decays a distance l away at D , then the proper decay time is $t = (m/c)(l/p)$. The potential time is $T = (m/c)(L/p)$, where L is the distance from P along the line of flight to the intersection with one of the surfaces that define the fiducial volume. The fiducial volume used here is the same as that used in the cross section determination. The same cut-off correction of 3 mm as discussed previously is applied to l and L . This excludes two observed Λ events with decay lengths less than 3 mm.

The average potential time in this experiment is 16 times the average decay time, and a good lower limit for the lifetime is provided by the average decay time. Thus 121 well-measured Λ -production-and-decay origins provide an average decay time $\bar{t} = (3.12 \pm 0.34) \times 10^{-10}$ sec where the 11% error is combined from the statistical uncertainty

of 9% and a random momentum error of 6%. Most of the momentum error is due to multiple scattering. An integral decay plot is shown in Fig. 14. The decay curve drawn corresponds to the observed average decay time.

The maximum-likelihood estimate of the mean life²⁵ provides an additive correction to the mean decay time of $(1/N) \sum_{i=1}^N T_i / (e^{-\lambda T_{i-1}})$ which is approximately $(1/N) \sum_{i=1}^N T_i e^{-\lambda T_i}$ for $\lambda T_i \ll 1$. Here N is the number of events. One can estimate this correction by assuming a rough value for $\lambda = \tau^{-1}$ and evaluating the above term. If the value $\tau = 3 \times 10^{-10}$ sec is assumed, the correction amounts to 4% of \bar{t} and the corrected mean life is $\tau_{\Lambda} = (3.24 \pm 0.36) \times 10^{-10}$ sec.

Although the value for τ_{Λ} reported here is high, it agrees with the values generally found in cosmic rays¹⁴ and also that obtained in the Berkeley bubble-chamber experiments.



MU-17134

Fig. 14. Integral decay plot of 121 Λ decays (uncorrected for losses). The slope drawn is the mean decay time.

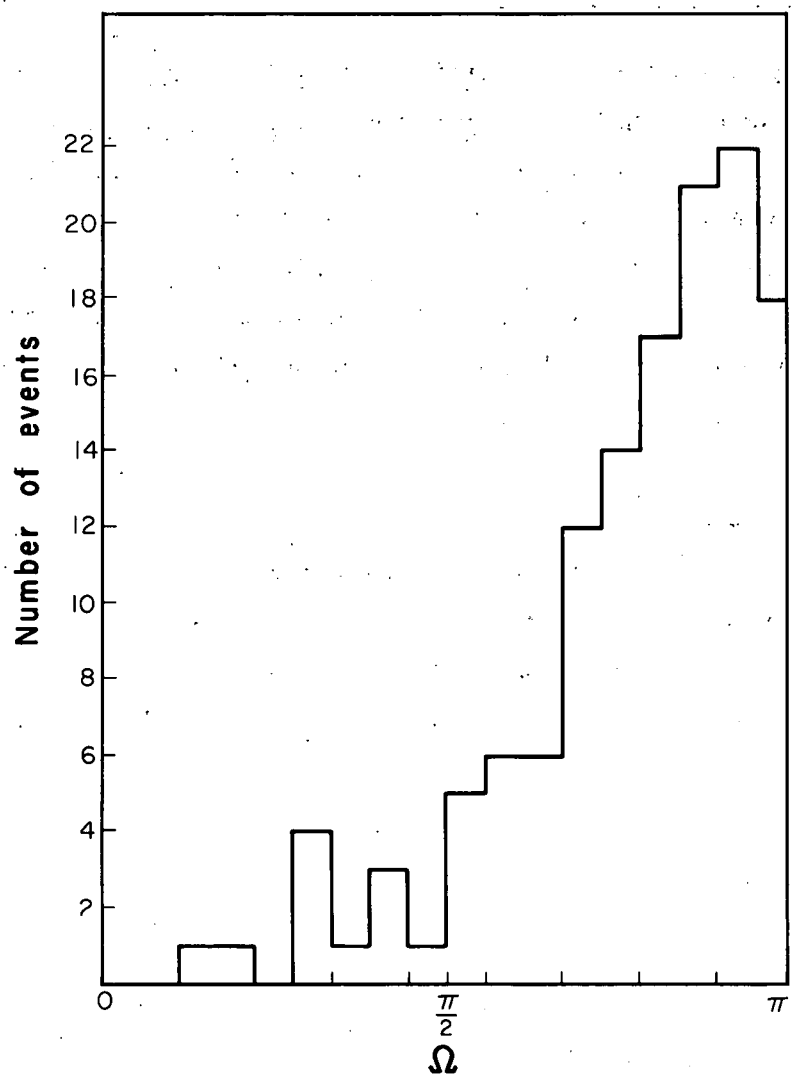
Production Angular Distributions

The Center-Of-Mass Distribution

The angular distribution for neutral-hyperon production peaks backwards for production in the vicinity of threshold. The events observed at 5 Bev exhibit the same form. Figure 15 shows the production angular distribution for the observed Λ particles. Here Ω is the center-of-mass production angle when the production system is assumed to be a 5-Bev pion incident upon a proton at rest. No distinction can be made between directly produced Λ 's and those arising from Σ^0 production.

The Laboratory Distribution

The Y^0 -production angular distribution in the laboratory system is largely forward as shown in Fig. 6. Here Ω_L is the polar angle of the outgoing Λ with respect to the beam axis. There were no Λ hyperons observed to travel backward in the laboratory system.



MU-17120

Fig. 15. The Λ production center-of-mass angular distribution.

Decay Angular Distributions

The Up-Down Distribution

The up-down distribution with respect to the Λ -hyperon production plane depends on two conditions: first, that the hyperons have spin and are polarizable, and second, that parity is not conserved in their decay.²⁶ The Λ has a preferred decay orientation with respect to its spin. In particular the π^- comes off preferentially "up" when "up" is defined as $\hat{p}_i \times \hat{p}_\Lambda$. The vectors are unit vectors associated respectively with the incident-pion momentum and the outgoing- Λ -particle momentum. The original interest in this distribution for hyperons was to test parity conservation for decay processes that did involve a neutrino.

The description of this decay asymmetry follows that previously given in the literature.²⁷ The pseudoscaler $\xi = \hat{p}_\pi \cdot \hat{p}_i \times \hat{p}_\Lambda$, where all quantities are measured in the laboratory system, was examined for 135 Λ decays and yielded a $\bar{P}_1 = \frac{3}{N} \sum_{i=1}^3 \xi_i \pm \sqrt{\frac{3}{N}} = 0.12 \pm 0.15$. Here \bar{P}_1 is the component of hyperon polarization along $\hat{p}_i \times \hat{p}_\Lambda$ averaged over all production angles, and a is a constant that represents the degree of parity violation. The constant a has been measured.²⁸ Consequently the up-down asymmetry measured here represents a measure of the hyperon polarization for the entire sample of Λ hyperons produced in hydrogen and carbon (Fig. 16). There is no indication of an up-down decay asymmetry.

Selection of those Λ particles originating from production stars with fast prongs should represent Λ 's produced in direct pion-nuclear interactions, and for this sample we obtain $a\bar{P}_1 = 0.12 \pm 0.21$ which indicates the same lack of up-down decay asymmetry.

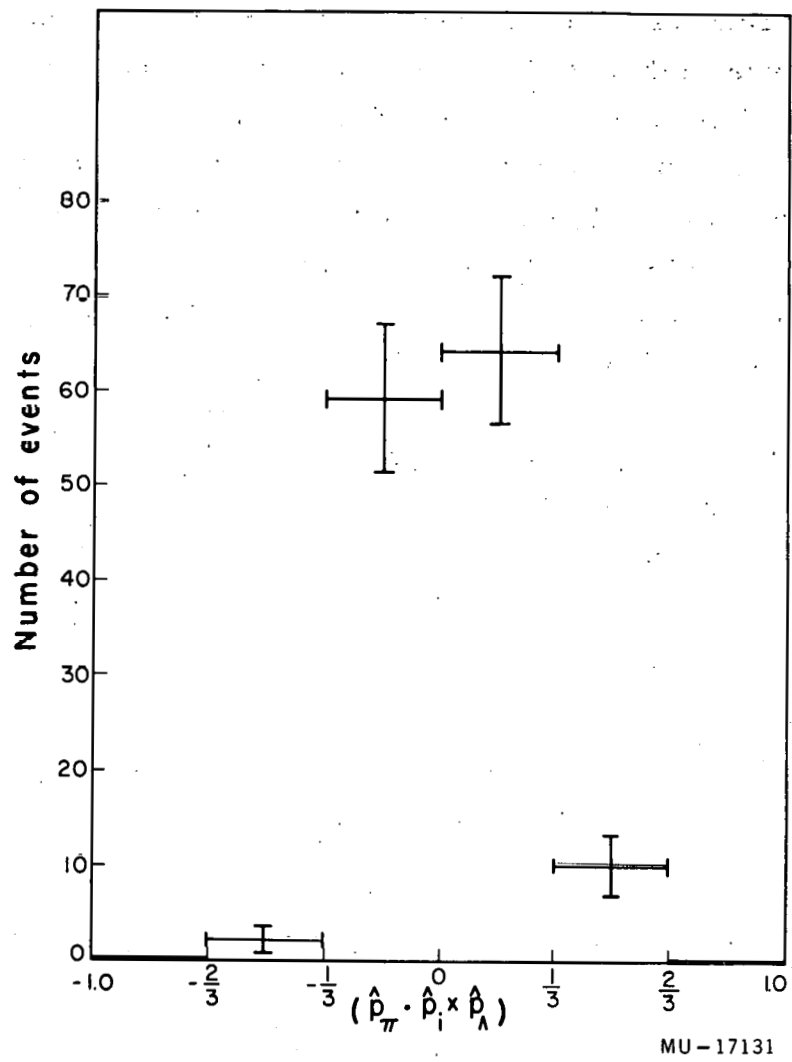


Fig. 16. Distribution of $P_\pi \Lambda$ decays with respect to the production plane.

The Fore-Aft Distribution

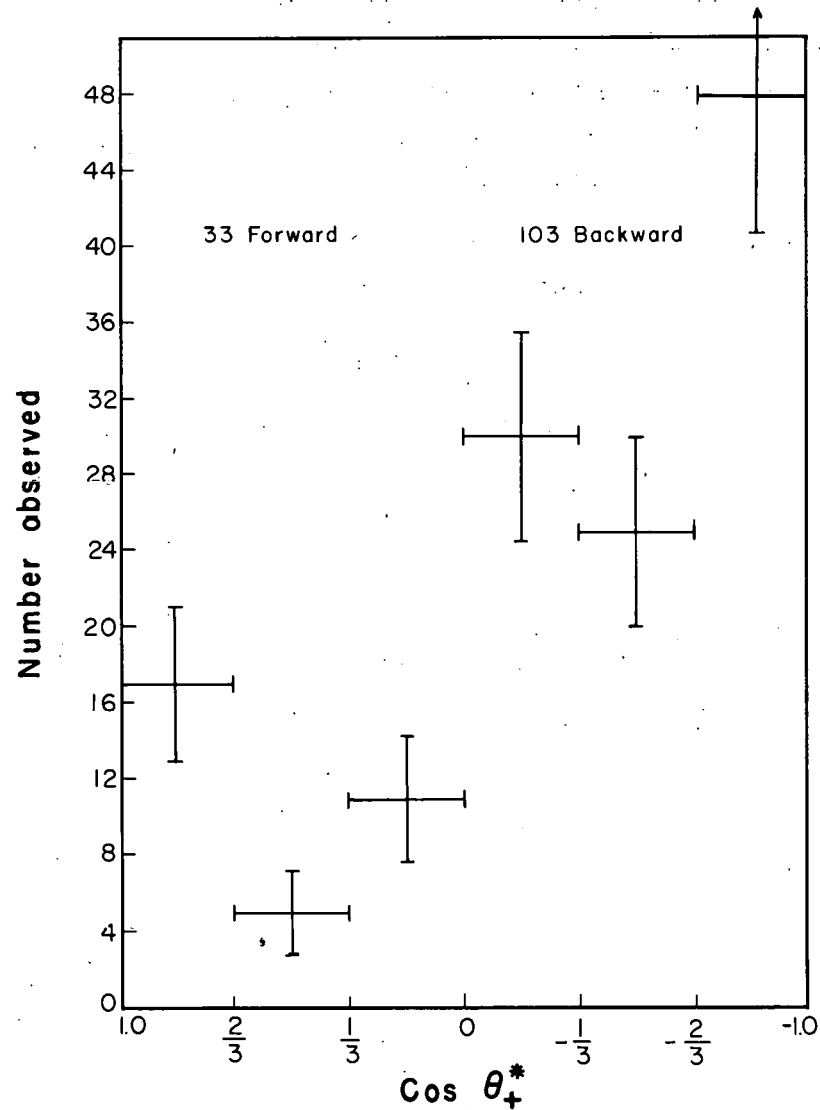
The decay angular distribution in the Λ rest frame with respect to the Λ line of flight has recently been of interest.²⁹ Observations of Λ decays arising from associated production by π^- -p interactions near threshold yield a symmetrical fore-aft decay distribution. However, several experiments in which strange particles are produced by high-energy particles incident on complex nuclei have shown a fore-aft asymmetry for the observed Λ decays.³⁰ These experiments all agree on the sign of the effect, which is that the proton goes preferentially backward in the Λ rest frame. This experiment yields the same result. Figure 17 shows the distribution in the decay angle (θ_+^*) that the proton makes with the Λ line of flight in the decay rest frame. In this distribution only those V's positively identified as Λ hyperons are tabulated. There is a definite backward peaking for all identified Λ particles. This distribution is undoubtedly biased by the fact that slow protons are most easily identified, and therefore those going backward enrich this sample.

In an attempt to overcome this bias, all events that were consistent with being Λ hyperons are plotted in Fig. 18. These include all events where it was impossible to distinguish between Λ and θ particles but not those where the decay was positively identified as a θ . This curve shows a definite asymmetry. The asymmetry is estimated from

$$a\bar{P}_3 = 3/N \sum_{i=1}^N (\cos \theta_+^*)_i \pm \sqrt{3/N} = -0.31 \pm 0.12,$$

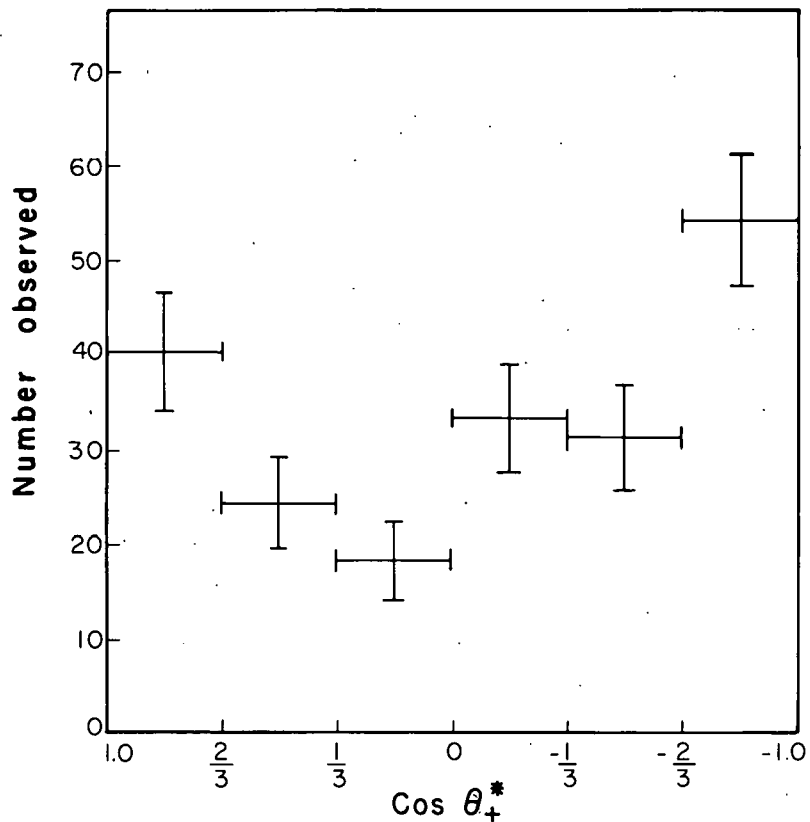
where \bar{P}_3 is the component of hyperon polarization along its direction of motion averaged over all center-of-mass production angles.

To make this distribution symmetric would require an error 2.5 times the statistical error. A similar curve (Fig. 19) was drawn for those V's positively identified as θ particles. The value of $a\bar{P}_3$ for this distribution is 0.04 ± 0.13 , showing no evidence for asymmetry.



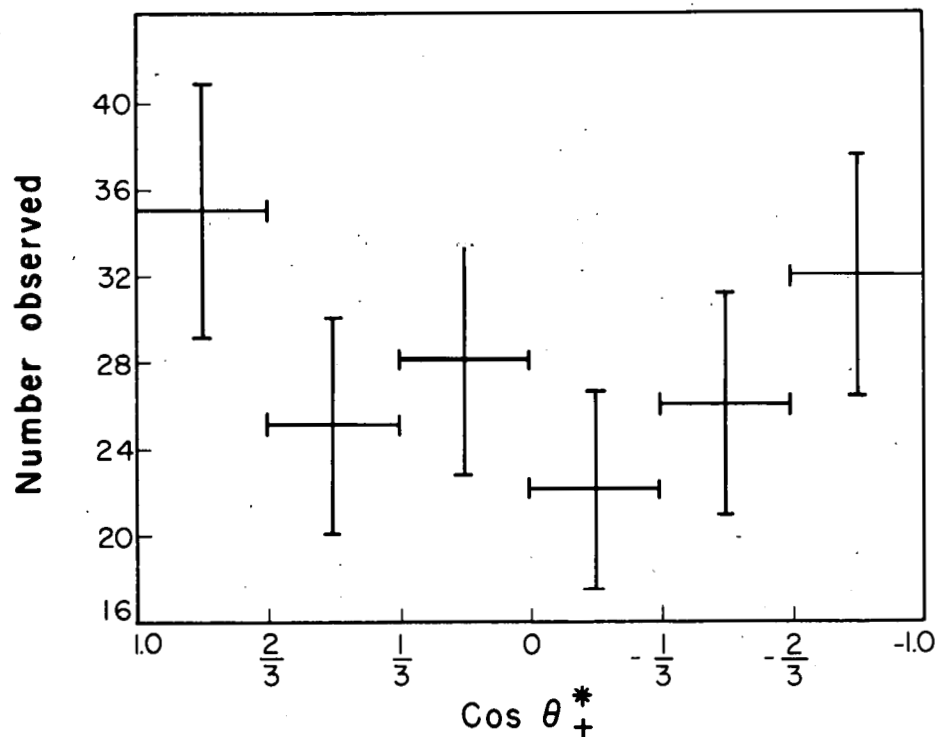
MU-17123

Fig. 17. Proton angular distribution in Λ rest frame with respect to the Λ line of flight.



MU-17129

Fig. 18. Combined distribution for Λ and $\Lambda-\theta$ set of the positive-prong's decay angle with respect to the V^0 line of flight. A Λ decay rest frame is assumed.



MU-17130

Fig. 19. The π^+ angular distribution in θ^0 rest frame with respect to θ^0 line of flight.

If this particular asymmetry for the combined distribution is real, it implies that the observed sample is longitudinally polarized along its direction of motion. If one assumes the Λ hyperon was produced directly, this implies that parity was not conserved in the direct production. Presumably Σ^0 production is contributing to the observed sample of Λ particles. Gatto has shown that if the decay $\Sigma^0 \rightarrow \gamma \Lambda$ conserves parity and the direction of the Λ relative to the Σ^0 is not observed, then the Λ arising from Σ^0 decay will exhibit a polarization dependent on the polarization state of the Σ^0 .³¹ Gatto has also shown that Λ hyperons arising from Ξ decay can exhibit a fore-aft asymmetry. This should have a negligible effect on the distribution, since so few Ξ hyperons are observed.

A possible explanation is that the combined distribution in θ_{+}^* is symmetric but that the apparent asymmetry results from a bias in calculating θ_{+}^* . A check on the consistency of the IBM-650 program that yields θ_{+}^* is afforded by Fig. 20 which is a family of curves of constant decay opening angle as functions of $P_1 = P_{+}$ and $P_2 = P_{-}$, the momentum of the positive and negative prongs, respectively. For a particular Λ decay the measured values of (P_{+}, P_{-}) define a point on some curve corresponding to Λ -decay opening angle. If it falls to the right of the heavy dotted line ($\cos \theta_{+}^* = 0$), the proton goes forward, and if to the left, the proton goes backward. Now consider the distribution for the identified Λ sample (Fig. 17). For this distribution 103 protons go backward and 33 forward. By the use of the measured (P_{+}, P_{-}) for these same events and of the curves of Fig. 20, the same division of 103 backward and 33 forward protons is found. Thus the calculation is consistent with respect to the fore-aft distribution, and one may assume that the asymmetry is not due to a calculational bias.

If one assumes that parity is conserved in production, then a $\bar{P}_3 = -0.31$ represents a fluctuation greater than 2.5 standard deviations. Furthermore the above discussions show that it is highly unlikely that the asymmetry for the combined distribution (Fig. 18) is due to bias. Therefore one must conclude that the combined sample is longitudinally

polarized with the same probability that $(31 \pm 12)\%$ is not a fluctuation from an isotropic distribution.

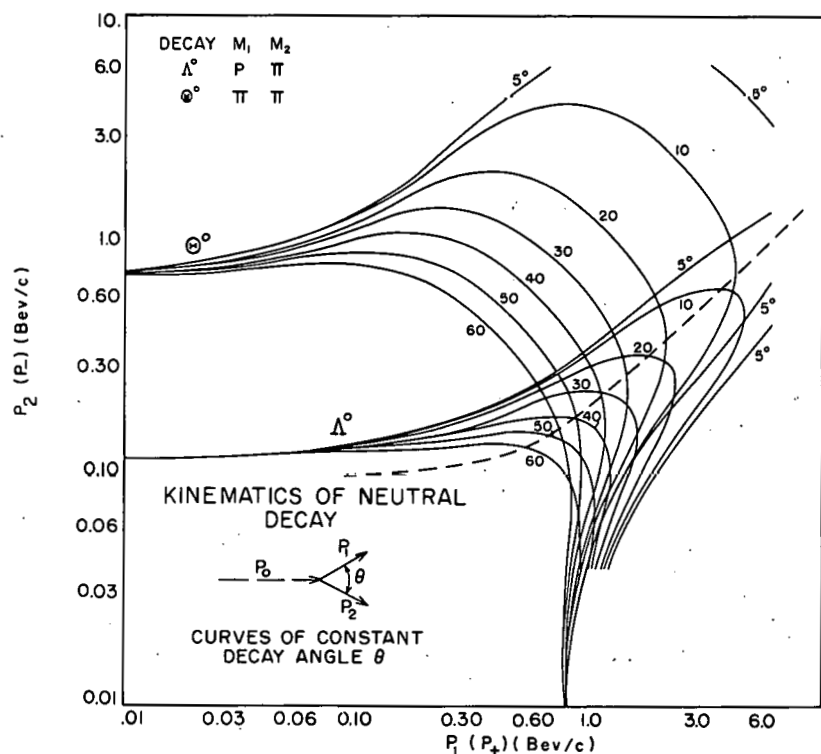
The conclusion is that within the statistical limits of this experiment there is an indication that parity is not conserved in the production of the Λ hyperons.

The Λ Momentum Distribution

The laboratory momentum distribution for all the observed Λ^0 particles is shown in Fig. 20. The solid curve is the observed distribution. The dotted curve represents the corrected distribution weighted according to Gayther and Butler.¹⁹ The distribution peaks around 500 Mev/c which is consistent with the observed backward peaking in the production center of mass.

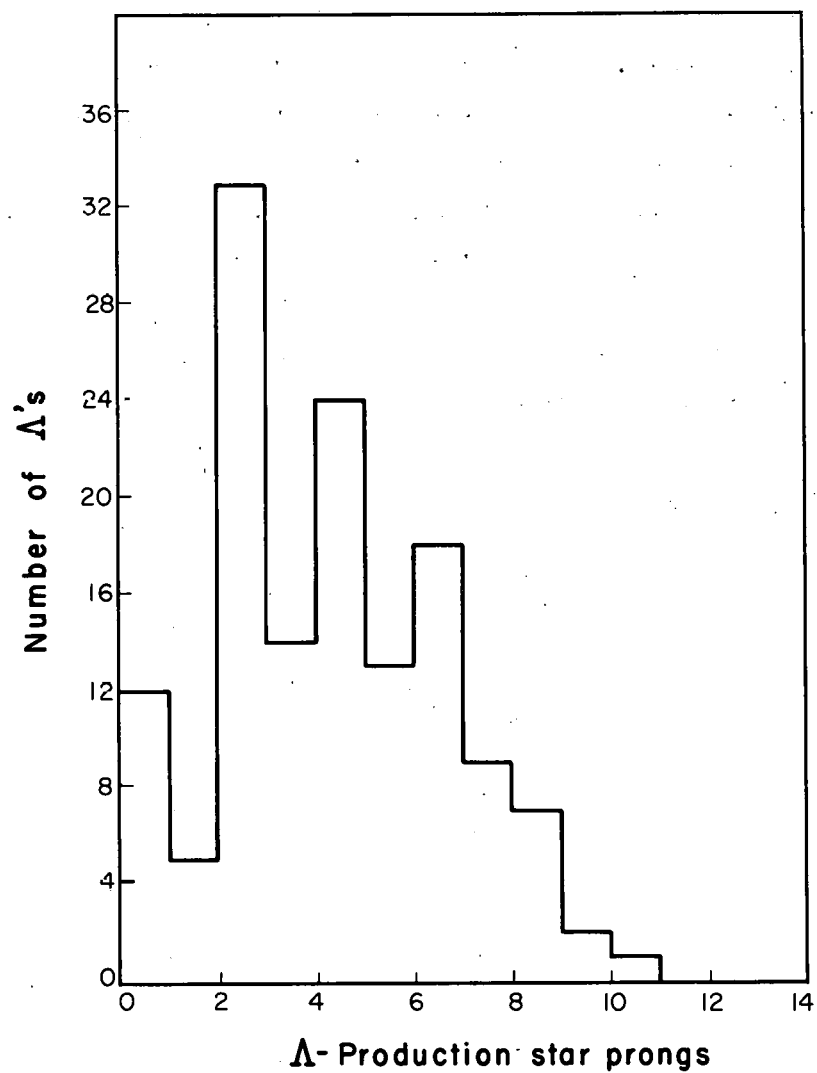
Production-Star Prong Distribution

The prong distribution for all production-star types associated with an identified Λ is shown in Fig. 21. The average prong multiplicity is 3.8 and the maximum observed was 10 prongs.



MU-17186

Fig. 20. The V^0 -decay opening angle versus momenta of decay products.



MU-17122

Fig. 21. Distribution of Λ -production star prongs.

ACKNOWLEDGMENTS

The advice and support of Professor Wilson M. Powell throughout my student tenure and especially during the execution of this project is recorded with a warm sense of gratitude.

Drs. William B. Fowler, Richard L. Lander, Robert W. Birge, and Robert E. Lanou have contributed much to this project in their continued assistance and personal encouragement.

Data reduction was handled by the data-processing group ably guided by the indispensable man, Howard White.

Some work was done in conjunction with John Shonle whose contributions are appreciated. Many other members of the Cloud Chamber Group gave much technical assistance.

This work was performed under the auspices of the U. S. Atomic Energy Commission.

APPENDIX

Table of lifetimes*

Group	Technique [†]	No. of events	$\tau_\Lambda \times 10^{10}$ sec
Berkeley(K-capture)	H. B. C.	76	2.95 ± 0.4
Berkeley(assoc. - prod.)	H. B. C.	340	3.04 ± 0.35
Columbia	H. B. C.	454	
Pisa	P. B. C.		2.29 ± 0.15
Bologna			-0.13
Columbia	C. C.	74	2.75 ± 0.45
Jungfraujoch	C. C.	40	3.04 ± 0.78
Michigan	P. B. C.	61	2.08 ± 0.46
Massachusetts Institute of Technology	C. C.	200	2.4 ± 0.2
Mean lifetime		$\tau_\Lambda =$	2.60 ± 0.16
			-0.14

* From Prog. 958 Annual International Conference on High-Energy Physics at CERN (CERN, Geneva, 1958), p. 220.

[†]Abbreviations used are:

H. C. B. hydrogen bubble chamber

P. B. C. propane bubble chamber

C. C. cloud chamber.

BIBLIOGRAPHY

1. G. D. Rochester and C. C. Butler, *Nature* 160, 855 (1947).
2. Fowler, Shutt, Thorndike, and Wittemore, *Phys. Rev.* 93, 861 (1954); *ibid* 98, 121 (1955).
3. Fowler, Shutt, Thorndike, and Wittemore, *Phys. Rev.* 97, 797 (1955).
4. Abraham Pais, *Phys. Rev.* 86, 663 (1952).
5. Murray Gell-Mann, *Phys. Rev.* 92, 833 (1953); T. Nakano and K. Nishijima, *Prog. Theoret. Phys.* 10, 581 (1953).
6. Brown, Glaser, Perl, *Phys. Rev.* 108, 1036 (1957); F. Eisler et al., *Nuovo cimento* 10, 468 (1958).
7. Alvarez, Bradner, Falk-Variant, Gow, Rosenfeld, Solmitz, and Tripp, *Nuovo cimento* 5, 1026 (1957).
8. M. Gell-Mann and A. Pais, *Phys. Rev.* 97, 1387 (1955); A. Pais and O. Piccioni, *Phys. Rev.* 100, 1487 (1955); Richard L. Lander, *The Neutral K Meson as a Particle Mixture* (Thesis). UCRL-3930 Sept. 1957.
9. Lande, Booth, Impeduglia, and Lederman, *Phys. Rev.* 103, 1901 (1956).
10. Lee, Steinberger, Feinberg, Kabir, and Yang, *Phys. Rev.* 106, 1367 (1957); Crawford, Cresti, Good, Gottstein, Lyman, Solmitz, Stevenson, and Ticho, *Phys. Rev.* 108, 1102 (1957); F. Eisler et al., *Phys. Rev.* 108, 1353 (1957).
11. T. D. Lee and C. N. Yang, *Phys. Rev.* 109, 1755 (1958); R. K. Adair, *Phys. Rev.* 100, 1540 (1955); F. Eisler et al., *Nuovo cimento* 7, 222 (1958).
12. Maenchen, Fowler, Powell, and Wright, *Phys. Rev.* 108, 850 (1957).
13. Baxter H. Armstrong, *Analysis of V Particle Decays at Bevatron Energies* (Thesis), UCRL-3470, July 1956.
14. See Proc. 1958 Annual International Conference on High-Energy Physics at CERN, Geneva 1958 for a survey of lifetimes.
15. Powell, Fowler, and Oswald, *Rev. Sci. Instr.*, 29, 874 (1958).

16. Fowler, Powell, and Shonle (Nuovo cimento, in press).
17. R. P. Feynman and M. Gell-Mann, Phys. Rev. 109, 193 (1958); Nordin, Orear, Reed, Rosenfeld, Solmitz, Taft, and Tripp, Phys. Rev. Lett. 1, 380 (1958).
18. Eisler, Plano, Samios, Schwartz, and Steinberger, Nuovo cimento 5, 1700 (1957).
19. D. B. Gayther and C. C. Butler, Phil. Mag. 46, 467 (1955).
20. The value of λ_T was determined to be 200 cm in propane.
21. N. Frederick Wikner, Nuclear Cross Sections for 4.2-Bev Negative Pions (Thesis), UCRL-3639, January 1957.
22. Eisler, Plano, Prodell, Samios, Schwartz, Steinberger, Bassi, Bonelli, Puppi, Tanaka, Waloschek, Zoboli, Conversi, Franzini, Manelli, Santangelo, and Siverstrini, Nuovo cimento 10, 468 (1958).
23. Blumenfeld, Chinowsky, and Lederman, Nuovo cimento 8, 296 (1958).
24. A good discussion is found in the review article by C. Franzinetti and G. Morpurgo, Nuovo cimento Suppl. 6, (1957).
25. W. L. Alford and R. B. Leighton, Phys. Rev. 90, 209 (1953).
26. T. D. Lee and C. N. Yang, Phys. Rev. 104, 254 (1956).
27. Lee, Steinberger, Feinberg, Kabir, and Yang, Phys. Rev. 106, 1367 (1957).
28. Boldt, Bridge, Caldwell, and Fal, Phys. Rev. Lett. 1, 266 (1958).
29. Crawford, Cresti, Good, Solmitz, and Stevenson, Phys. Rev. Lett. 1, 209 (1958); ibid. 2, 11 (1959); and references cited by them.
30. See the discussion of Cooper, Filthuth, Montanet, Newth, Petrucci, Salmcron, and Zichichi, Nuovo cimento 8, 471 (1958); Blumenfeld, Chinowsky, and Lederman, Nuovo cimento 8, 296 (1958) and references cited by them.
31. R. Gatto, Phys. Rev. 109, 610L (1958); ibid. Nuclear Physics 5, 183 (1958).

This report was prepared as an account of Government sponsored work. Neither the United States, nor the Commission, nor any person acting on behalf of the Commission:

- A. Makes any warranty or representation, expressed or implied, with respect to the accuracy, completeness, or usefulness of the information contained in this report, or that the use of any information, apparatus, method, or process disclosed in this report may not infringe privately owned rights; or
- B. Assumes any liabilities with respect to the use of, or for damages resulting from the use of any information, apparatus, method, or process disclosed in this report.

As used in the above, "person acting on behalf of the Commission" includes any employee or contractor of the Commission, or employee of such contractor, to the extent that such employee or contractor of the Commission, or employee of such contractor prepares, disseminates, or provides access to, any information pursuant to his employment or contract with the Commission, or his employment with such contractor.